

## Multi-Decadal Changes Of Mangrove Forest And Its Response To The Tidal Dynamics Of Thane Creek, Mumbai

Abdul Azeez.S<sup>1,2</sup>, Gnanappazham.L<sup>2</sup>, Muraleedharan K.R<sup>1\*</sup>, C Revichandran<sup>1</sup>, Sebin John<sup>1,5</sup>,  
Seena G<sup>1</sup>, Jubin Thomas<sup>3,4</sup>

1 CSIR-National Institute of Oceanography, Regional Centre, Kochi

2 Indian Institute of Space science and technology, Trivandrum

3 CSIR-National Institute of Oceanography, Regional Centre, Mumbai

4 ESSO-National Centre for Earth Science Studies, Trivandrum

5 India Meteorological Department (IMD), New Delhi

### Abstract

Mangroves are one of the world threatened ecosystems, which is protected and categorised under CRZ-I according to the Coastal Regulation Zone (CRZ) notification. The present study marked the decadal (1990-2017, Landsat series) change of mangroves and mapped the species distribution (2017, Sentinel-2) around Thane creek, Mumbai using SMLC with QGIS-SCP software. ADCIRC model was used to simulate the tidal flooding/ebbing towards mangroves, and the model was validated with the *in-situ* observation of tides and currents. From 1990 to 2017, the mangrove area increased from 79.14 km<sup>2</sup> to 154.5 km<sup>2</sup> and expanded towards landward and seaward regions. Between 2010 and 2017, there was a fluctuation in the mangrove area with ups and downs in their distribution caused by different climatic conditions and anthropogenic activities. The increase in built-up area was two times than mangrove area increase. The dominance of *Avicennia marina* species confirms the increased anthropogenic activity along the landward side. To understand the response of mangroves to the tidal dynamics, the model was simulated with two scenarios; *with mangroves* and *without mangroves*. In the absence of mangroves (*without mangroves*), Thane Creek demonstrated a perfect funnelling effect by increased tidal amplification with strong flood currents, resulting in severe coastal inundation and erosion. While *with mangroves*, tidal currents attenuated 80% of its magnitude and favoured the sediment deposition in mangrove areas, which further enhanced mangrove growth, thereby stabilising the coast. The present study has found that the mangroves in the Thane creek are in the saturation stage and reached the maximum growth towards the landward. The study envisages that the stakeholders should adopt a proper management plan for the restoration of mangroves. The highlight of the present study is the combination of satellite imagery and hydrodynamic modelling. Satellite imagery provides the estimated extent of the mangroves, and this information will be used when simulating the model, which provides maximum inundation and attenuation. The utilisation of LULC classification and ADCIRC model results would be helpful to examine the threatening built-up area due to the tidal inundation. The combination of satellite classification and hydrodynamic model findings will be decisive for management authorities towards the conservation and regeneration activities for a balanced mangrove-creek ecosystem.

**keywords:** Tides and currents, Mangroves, Remote sensing, Wetting and drying, ADCIRC .

## 1. Introduction

Mangroves are a taxonomic group of tropical trees and shrubs that grow in the intertidal saline or brackish water zone and act as a natural barrier to protect and stabilise the coastal region against erosion caused by storm waves conditions (Blankespoor et al., 2017; Chapman, 1971; Marois and Mitsch, 2015; Spalding et al., 2014; WCMC, n.d.; Wells and Ravilious, 2006). They have particular adaptations like salt resistance to survive such an environment (Kerr and Baird, 2007; Mitsch et al., 2015, 2009; Tomlinson, 1986) and cannot tolerate temperature below 0 °C in mid-tropical and polar areas (Duke et al., 2007). According to Tomlinson (1986), mangroves grow in a depositional environment with low wave energy. High waves prevent propagule establishment, expose the shallow root systems, and prevent the accumulation of fine sediments (Alappatt, 2008). Flood-ebb tidal dynamics serve as subsidies to mangrove systems, the constant alternation of standing water and then no water and fluctuations in salinity reduces competition from other vascular plants (Odum et al., 1982). In some areas, the tides carry the saltwater to the upstreams of the estuary against the outflow of freshwater, allowing mangroves to be established inland (Odum et al., 1982). The mangroves not only manage the daily rise and fall of tides but also slow the movement of tidal currents, reduce the transport of sediments and nutrients, and other pollutants, export organic carbon, and reduce sulphur compounds, and eventually immaculate the aquatic environment (Odum et al., 1982; Spalding et al., 2014; Tam and Wong, 1999).

Mangrove forests are highly productive ecosystems, which always provide many goods and services to the marine and human beings (Carugati et al., 2018). The global distribution of mangroves is about 150,000 km<sup>2</sup>, in which Southeast Asia possesses the largest and most diverse mangrove ecosystems (FSI, 2017) (Supplementary Fig. 1). Mangrove cover in India is approximately 4921 km<sup>2</sup> (~3% of the world's mangrove vegetation) and are mainly distributed along with the coastal belts of the Arabian Sea (Gujarat, Maharashtra, Goa, and Kerala) and Bay of Bengal (Pichavaram, Cauvery deltaic, Krishna-Godavari, Mahanadi, Bhitarkanika, and Sundarbans) (FSI, 2017) (Supplementary Fig. 2). The major deltaic mangrove forests of the Sunderbans in West Bengal cover about half of the mangroves in India (FSI, 2017). In addition, Bhitarkanika in Odisha is best known for the presence of 51-57 diverse mangrove species out of 114 species worldwide (Mandal and Naskar, 2008; Pattanaik et al., 2008; Tomlinson, 2016). The presence of mangrove forest in these areas not only protect the coast and adjacent human beings from sea level rise and high wave actions while simultaneously absorbing eight times more carbon dioxide from the atmosphere than any other ecosystem (carbon sequestration) (Donato et al., 2011). The FSI has been assessing mangrove forests using remote sensing data since 1987 (Giri et al., 2007).

Remote sensing is a cost-effective technique that plays a vital role in mapping and monitoring the long-term changes of mangroves and the mangrove species distribution (Dahdouh-Guebas et al., 2000; Nayak, 2002; Neukermans et al., 2008; Wang et al., 2003). Optical satellite imageries such as Landsat and Sentinel-2 with varying temporal and spatial (10 to 30 m) resolution are mostly available datasets for mapping mangroves. There are several studies carried out based on mangrove mapping using the satellite image classification techniques such as visual interpretation, supervised classification, unsupervised classification, neural network classification, object-based methods (Everitt et al., 2010; Ferreira et al., 2009; Giri et al., 2008; Mas, 2004; Parida and Kumar, 2020; Rakotomavo and Fromard, 2010; Roy et al., 2019; Selvam et al., 2003; Wang et al., 2004). A study by Dan et al., (2016) showed that the loss of mangroves in West Asia and Central Africa from 1988 to 2014 was about 16.9 %. At the same time, only 2.5 % has been reclaimed or replanted, while the overall mangroves in the Sundarbans have increased approximately by 900 km<sup>2</sup>. Decadal changes in the mangrove forests of Pichhavaram on the southeast coast of India have revealed that there was a loss of 4.71 km<sup>2</sup> of mangroves from 1970 to 1991 and a gain of 5.31 km<sup>2</sup> in 2011 (Gnanappazham and Selvam, 2011). Thus, studies of mangrove forests using satellite data are necessary, but it is limited to the decadal changes of the area, its extension, and monitoring, and also it restricts to provide the real-time hydrodynamic response of the ecosystem to the natural phenomena (tides, storm surges, cyclones, Tsunami, etc.). Tidal propagation induced by cyclones and Tsunami towards the coastal regions, mangroves, creeks, estuaries, and rivers has been a topic of interest to hydrologists for many years (Van Loon et al., 2016). Modelling the mangrove ecosystem becomes complicated due to the bathymetric variations, bottom friction, shoreline slope, narrow channels, and freshwater discharge from the rivers. Different numerical methods, algorithms, computer programs, and supporting software platforms are available to study coastal region hydrodynamics, including mangroves. Bunt et al., (1980) developed a finite-difference implicit numerical model, used to calculate the movement of water and sediments in the tidal creek surrounded by thickly vegetated mangrove swamps in Missionary Bay, North Queensland, Australia. This model shows that the density of mangrove vegetation determines the physical characteristics of the creek as the net downstream water current enhances the export of nutrients from mangrove swamps and is responsible for maintaining a deep self-scouring drainage channel. Several studies showed that wave attenuation strongly depends on the mangrove density, diameter of stem and roots, bathymetry, incident tides, and waves (Massel et al., 1999; Mazda et al., 2006, 1997a; Zhang et al., 2012). These studies confirm the importance of understanding the features of mangroves (area and density) during the simulation of a hydrodynamic model. Therefore, a combination of satellite and hydrodynamic modeling is essential for the study of mangroves concerning anthropogenic activity and climate change.

In recent scenarios, the mangrove hotspots facing climate change and land use/land cover (LULC) change due to various anthropogenic activities (Ghosh et al., 2020; Kathiresan, 2018; Parida et al., 2020). Natural factors such as erosion, waves, storms, hurricanes, and earthquakes gradually change the LULC of coastal areas (Kaliraj and Ch, 2012; Mujabar and Chandrasekar, 2013; Nayak, 2002; Short and Trembanis, 2004; Zhang, 2011). Almost 40% of mangrove cover in India has been lost during the last century due to urban development and overexploitation (Krishnamurthy et al., 2014; Polidoro et al., 2010; Sahu et al., 2015; Youdon, 2020). Awareness about the importance of mangroves gathered momentum after the Tsunami hit the Indian coast in 2004. The 2004 Indian Ocean Tsunami has severely affected the coastal premises of Asian and African countries economically and ecologically (Kathiresan and Rajendran, 2005), while the areas where the dense mangroves were available resulted in the savage of millions of people (Patel et al., 2014). Dense mangrove forest attenuates waves more effectively than low-density forest (Alongi, 2008; Mazda et al., 1997a, 1997b). One-third of India's population (~260 million) lives within 50 km of nine coastal states such as Gujarat, Maharashtra, Goa, Karnataka, Kerala, Tamil Nadu, Andhra Pradesh, Odisha, and West Bengal (Roy, 2019). Among the coastal states, Mumbai in Maharashtra is a highly populated and polluted coastal city in India, which is featured by Asia's largest industrial complex. The effluents from these industries adversely affect the aquatic ecosystem, especially mangroves. The presence of mangroves in Mumbai has an essential role in the functioning of marine and aquatic ecosystems, protecting adjoining human dwellings from natural hazards. Mangroves in Mumbai store 2,38,417 tonnes of carbon, primarily from pollutants released into the atmosphere by human activities (Hindustan Times 13<sup>th</sup> July, 2015), thereby sinking the atmospheric pollution and keeping better air quality compared with other metro cities like Delhi (WHO, 2014). Mumbai has probably lost 40% of all its mangroves in the past decade or so, mainly due to growing population pressure, construction and development activities, conversion to agricultural land and fish farms, besides the effect of industrial effluents (Everard et al., 2014). Mangrove cover in Maharashtra over three decades by the FSI showed a considerable increase since 1999 (approximately 108 km<sup>2</sup> in 1999 to 304 km<sup>2</sup> in 2017) (Supplementary Fig. 3). After the monsoon flood in Maharashtra in 2005, the Bombay High Court ruled to prevent any destruction of the city's mangroves, quoting India's Forest Conservation Act of 1980 and the Coastal Regulation Zone Notification, 1991. Currently, the situation is more vulnerable; Mumbai is cutting down mangroves even if the region is affected by extreme weather events (Youdon, 2020).

Thus, the present study is the first of its kind by combining the information of the Mangrove cover assessment using satellite imagery and the hydrodynamic response of the mangrove ecosystem using a numerical model. We propose that if we know the extent and long-term changes of mangroves, it

will be a valuable addition to the numerical simulation of inundation and attenuation of waves and currents into the mangrove ecosystems and human settlements. Therefore the present study focus on the Thane creek, Mumbai, West coast of India with the objectives a) LULC change from 1990 to 2017, Change detection of mangrove cover from 1990 to 2017, and its species-level distribution for the year 2017, and b) Tidal dynamic response of mangroves using Advanced Circulation (ADCIRC) model.

## **2. Materials And Methods**

### **2.1 Study Area**

Mumbai is the most populated city in India, with 12.5 million as per the Census of India (2011) and United Nations report (2012). The city has several rivers and creeks, the main entrance being Thane Creek, and is surrounded by mangroves along both banks. Thane Creek, Mumbai, India is a shallow funnel-shaped semi-enclosed water body situated between latitudes  $18^{\circ} 48'$  to  $19^{\circ} 12'$  N and longitudes  $72^{\circ} 48'$  to  $73^{\circ} 00'$  E (Fig. 1). High hills (Kanheri, Yeur, and Parsik with maximum elevation of 450 m, 450 m, and 300 m respectively) on one side and submersible marsh and associated mangroves (elevation ranging from 1 to 3 m) along Thane creek particularly divided the terrain (Pradhan and Latkar, 2007). The region receives an average rainfall of 253.3 cm, and the majority occurs during July and August (Sahana et al., 2019). This creek is connected to the Arabian Sea in the southwest region and connected with the Ulhas river on its northern side with the narrow (average width  $< 200$  m) and shallow channel (average depth  $< 2$  m) and two islands viz, Elephanta and Jawahar Dweep at its southern side. Climatological river discharge data showed that Ulhas river has the maximum freshwater discharge of  $1300 \text{ m}^3/\text{sec}$  during July, followed by Amba river ( $500 \text{ m}^3/\text{sec}$ ) and Bhagwati river (less than  $100 \text{ m}^3/\text{sec}$ ) (India Water Resources Information System, <https://indiawris.gov.in/wris/#/>) (Supplementary Fig. 4). Mixed semidiurnal tide with an average amplitude of 2.5 m (mean tidal range 5 m) (Chouksey et al., 2004; Nayak and Balaji, 2016) during spring propagates to the creek through a 12 km wide and 12 m deep inlet area. The circulation pattern showed maximum velocities during neap and spring tide are 0.4 and 1.5 m/s, respectively (Naidu and Sarma, 2001).

The prevailing current enhances the annual sediment load at the central part of the creek to  $0.84 \times 10^6 \text{ m}^3$ , and the sediment is spread over the  $240 \text{ km}^2$  area of the creek with a sedimentation rate of 4 mm/year (Sastry, 1971), which is a major cause of continuous dredging in the creek's navigation channel (from creek mouth to port premises) (Thomas et al., 2019). The water quality of Thane creek is affected by vast quantities of wastewater of different varieties discharged from industries located on both banks of the creek main channel (Naidu and Sarma, 2001; Vijay et al., 2014). It is estimated that

$3.5 \times 10^8$  and  $1.8 \times 10^8$  L are discharged daily into the creek as domestic and industrial wastewater, respectively (Zingde et al., 1989). The environmental status report of the Mumbai metropolitan region (MMRDA) prepared by The Energy and Resources Institute (2015) showed that only two or three rivers produce freshwater while others are highly polluted and used as drainage systems (Supplementary Table 1). Industrial effluents, sewage, and garbage dumping have significantly degraded the creek, and it is essential to study the mangroves and creek tidal dynamics for the regeneration of the ecosystem. The present study deals with long-term Spatio-temporal changes of the mangroves (1990, 2000, 2010, and 2017) in the Thane creek, Mumbai, and associated tidal dynamics. The present study has adopted several datasets and methods (Fig. 2 and Table 1), such as satellite imagery analysis with ground-truthing and hydrodynamic model simulation, and is described in the following sections.

## **2.2 *In-situ* observations**

Water level and currents time-series measurements were conducted in Thane creek at three locations S1 (Colaba from 15<sup>th</sup> January 2013 to 18<sup>th</sup> February 2013), S2 (BARC, Trombay for water level from 16<sup>th</sup> January to 18<sup>th</sup> February 2013, and for currents from 16<sup>th</sup> January to 22<sup>nd</sup> January 2013), and S3 (Vashi from 17<sup>th</sup> January to 18<sup>th</sup> February 2013) (Fig. 1). Water levels were recorded at 10 minutes intervals using the Aanderaa Seaguard water level recorder. Aanderaa Seaguard RCM current meters were used to record current speed at 10 minutes intervals.

## **2.3 Satellite image processing and classification**

Ortho-rectified cloud-free (cloud cover < 10 %) Landsat series and Sentinel-2 images used for LULC, change detection of mangroves, and species-level classification. All Landsat and Sentinel-2 data were pre-processed to improve image quality, including atmospheric and geometric correction, layer stacking, and image enhancement. Pre-processing and further analyses (classification and accuracy assessment) of satellite imageries were performed using QGIS (version 2.18) Semi-Automatic Plugin (SCP) software (QGIS Development Team, 2018). A Supervised Maximum Likelihood Classifier (SMLC) (Richards, 2013) was employed to delineate the LULC for the years 1990, 2000, 2010, and 2017. The SMLC method uses a training dataset, which assigns a pixel to a specific class based on its maximum possible occurrence in that class (Eastman, 2009). The ground truth data obtained from the Google Earth Engine (GEE) was used to create training data for the classification; GEE provides a large amount of freely available satellite imagery (Shelestov et al., 2017). Mainly, five classes are distinguished, including water bodies, mangroves, other vegetations, built-up area, and remaining land regions. This step provides LULC of Thane creek from 1990 to 2017 with 30 m spatial resolution. For

change detection of mangroves, only mangrove regions were extracted from the LULC maps for the years 1990, 2000, 2010, and 2017. Finally, four different periods were overlaid on one another to detect the mangrove forest change (growth and degradation with 30 m resolution) between 1990 to 2017.

Sentinel-2 (10 m resolution bands) cloud-free imagery with the SMLC method is used for mangrove species mapping. The initial step is to classify mangroves and non-mangrove areas using ground truth data from GEE. Then extract the mangroves and convert them into polygon shapefile. To reduce the overlapping of other classified pixels, we performed a subset (section of original satellite image) function on Sentinel-2 data with a converted polygon shapefile, which will rebuild the Sentinel-2 image only with mangroves. Then executed SMLC on the subsetted image with the ground truth information from Kantharajan et al., (2018). Further, we created a training dataset and classified the most abundant mangrove species like *Bruguiera cylindrica*, *Sonneratia apetala*, *Avicennia marina*, and *Acanthus ilicifolius*. This step will provide the mangrove species distribution map for the year 2017 with a spatial resolution of 10 m.

Accuracy assessment is a vital step in any classification scheme, which compares the classified image with ground truth/reference/observations and quantitatively determines the efficiency of the pixels in a satellite image is clustered into the correct class or not (Behera et al., 2021; Regression, 2016). The present study used the kappa coefficient of classification, which indicated the actual agreement between the classified image and ground truth data and interpreted using the guidelines by Landis and Koch, (1977). The value of the kappa coefficient lies between 0 and 1, in which 0.01-0.20 slight; 0.21-0.40 fair; 0.41-0.60 moderate; 0.61-0.80 substantial; 0.81-1.00 almost perfect classification (Landis and Koch, 1977). The kappa coefficient (K) is calculated using the equation (Cohen, 1960),

$$K = (P_0 - P_e) / (1 - P_e) \text{ ----- (1)}$$

where  $P_0$  is the proportion of cases correctly classified and  $P_e$  is the expected proportion of cases correctly classified by chance.

#### **2.4 ADCIRC hydrodynamic modelling of Thane creek**

The ADCIRC is a two-dimensional, depth-integrated, barotropic time-dependent longwave, hydrodynamic circulation model (Luettich and Westerink, 1995). The equations have been formulated using the traditional hydrostatic pressure and Boussinesq approximations and discretised in space using the Finite Element (FE) method and in time using the Finite Difference (FD) method on an unstructured grid. It can be realistic to computational domains encompassing the deep ocean, continental shelves, coastal areas, and estuarine and creek systems. Unstructured grids are versatile to the highly complex geometry include many narrow channels and streams. Three-dimensional finite

element grids were created using an open-source Mesh Generator (GMSH version 3.0), with a built-in Computer-aided design (CAD) engine and post-processor developed by Geuzaine and Remacle (2009). The grids were connected with open boundaries, mainland boundaries, and islands. While SRTM (Shuttle Radar Topography Mission), CARTOSAT-1 (Cartography and Satellite), and GEBCO (General Bathymetric Chart of Oceans) data sets were used for land elevation and coastal water depth delineation purposes (Table 1). Incorporating topography data into the model domain was a tedious process, which often led to the instability of the model due to a small error in the computational grid. The Bathymetry of Thane creek was digitised using the high-resolution (10 to 100 m) bathymetric chart provided by the Maharashtra Maritime Board (MMB) for the year 2009 to 2012 (Thomas et al., 2019). Bathymetry and land elevation data were interpolated to the mesh using the Inverse Distance Weighted (IDW) method (Lu and Wong, 2008) (Supplementary Fig. 5). Five unstructured grids and the model control parameter files were created for the years 1990, 2000, 2010, 2013, and 2017 (Fig. 3) to run the ADCIRC model with the wetting and drying effects. When creating the grid, we included the mangrove area from the classification. The model time step set to the lowest Courant-Friedrichs-Levy (CFL) value in the domain (Hill, 2007), which states that

$$\frac{\Delta t}{\Delta x} \sqrt{gh} < CFL \text{-----} (2)$$

Where,

- $\Delta t$  is the simulation time step
- $\Delta x$  is the length between grid elements
- $g$  is the acceleration by gravity
- $h$  is the depth of water

Tidal forcing from the open boundary with a time step of one second initiates the model simulation. Tidal constituent data (13 components) obtained from the Global Tide LeProvost database (LeProvost database, 2008) were used to force tide from the open boundary. Wetting and drying were introduced in this model with an appropriate friction coefficient to analyse the water inundation in mangrove regions. To achieve accurate model results for the validation procedure, bottom frictional coefficients of 0.005 (depth > 10 m), 0.02 (depth < 10 m), and 0.02 to 0.2 (for mangroves) applied to the entire model domain. Bathymetry adjustment and optimisation of the various modeling parameters, including friction coefficient and wetting/drying, were undertaken until a satisfactory correlation between the model and observed tide data has achieved. The model operated in two scenarios, 1) *with mangroves* and 2) *without mangroves* (van Maanen et al., 2015). *Without mangrove* is simulated for an



experimental case only for the year 2017. In *without mangrove* condition, mangrove regions were completely removed, and the outputs compared with the actual scenario where mangroves were distributed over the domain as per the remote sensing data. The outputs of the ADCIRC model (tide and current) were stored in ASCII format and visualised using MATLAB tools. Finally, a validity check was performed to measure the model prediction accuracy. Model validation compares the simulated model output and the *in-situ* observations, which provides sufficient reliability to model the real-time scenario. For validation purposes, the model was simulated for the year 2013 and compared the results with available *in-situ* measurements of tides and currents at three locations, S1, S2, and S3. We have calculated correlation coefficient squared ( $R^2$ ), Index of agreement (IA), and root mean square error (RMSE), which provides the statistical summary of the model performance.

### 3. Results

#### 3.1 LULC mapping and change detection of mangroves

In the Landsat and Sentinel-2 imageries, mangroves can be characterised visually through combinations of bands (Khawfany et al., 2017). The true-colour combination of bands 3-2-1 (Red-Green-Blue) showed that mangroves appear to have a darker green than other vegetation (Fig. 4a). On the other hand, a false-colour combination of bands 5-3-2 (SWIR1-Red-Green) (Fig. 4b) and 4-5-6 (NIR-SWIR1-TIR) (Fig. 4c) represents mangroves as darker red and striking orange hue, respectively. In the Sentinel-2 image, a band combination of 4-3-2 (Red-Green-Blue) was used for true-colour composite (visualisation is same as Fig. 4a) and 8-4-3 (NIR-Red-Green) used for false-colour composite (visualisation is same as Fig. 4b). The study results focus on two classes: mainly mangroves and the built-up area. The classified LULC map for 1990, 2000, 2010, and 2017 along the Thane creek has been presented in Fig. 5. LULC mapping from 1990 to 2017 showed that the area of mangroves has increased from 79.14 km<sup>2</sup> to 154.5 km<sup>2</sup>, which includes very dense, moderately dense, and open mangroves. The total area of mangroves increased by 75.36 km<sup>2</sup> from 1990 to 2017. The built-up area has shown a dramatic increase since 1990. A total built-up area of 145.56 km<sup>2</sup> (436.55 km<sup>2</sup> in 1990 to 582.11 km<sup>2</sup> in 2017) was increased around mangrove regions, which was two times than mangrove area increase. During the first phase of the study (1990 to 2000), the built-up area increased towards the hinterlands of Mumbai, after which the built-up area has increased in line with the mangroves. Between 2010 to 2017, the increase in mangroves and the built-up area was 9.68 km<sup>2</sup> and 41.73 km<sup>2</sup>, respectively. Fig. 6 demonstrates the growth and degradation of mangroves from 1990 to 2017. Imageries spanning from 1990 to 2017 have been stacked into a single image for change detection analysis, and the major seaward and landward change of mangroves were demarcated in the circle and rectangular box respectively. The results revealed that the majority of mangroves increased towards

the seaward side except at Karanja creek (landward extension). The highest increase of mangroves was observed in the western region of Thane creek's main channel. One of the notable factors is that the width of the creek decreases as the mangroves increase towards the seaward. The major degradation of mangroves occurred between 2010 and 2017; this destruction is attributed to the expansion of the built-up area (four times that of mangroves).

### **3.2 Mangrove species classification**

The distribution of mangrove species was mapped using the classification of Sentinel-2 with a spatial resolution of 10 m to understand which species are mostly dominated in Thane creek. There were four common types of mangrove species in the Thane creek system, each with distinct zonation patterns concerning tidal action and land elevation (Kantharajan et al., 2018; Vijay et al., 2005). Thane creek system has been dominated by *Avicennia marina* species along the seaward side (Fig. 7). Species like *Bruguiera cylindrica* and *Acanthus ilicifolius* were present adjacent to the mainland where the maximum reach of tidal water occurs. Thane creek's main channel showed the combination of high-density *Avicennia marina* and *Sonneratia apetala* species.

### **3.3 Accuracy assessment**

LULC classified maps, and mangrove species level mapping was compared with GEE data and Kantharajan et al., (2018). A total of 400 random pixels were selected for each year, out of which 240 pixels were used for the supervised classification, and the remaining 160 were used for the classification accuracy. The average accuracy of 87 %, 88 %, 93 %, and 94 % was obtained for the years 1990, 2000, 2010 and 2017 with a K value of 0.79, 0.86, 0.91 and 0.93 respectively (Table 2). Mangrove species classification has shown a relatively low accuracy of 66 %, with a K value of 0.64 (Table 2).

### **3.4 Tidal water dynamics in Thane creek (*with mangroves* and *without mangroves*) and model validation**

The ADCIRC model was set up with the appropriate initial-boundary settings to delineate the flood and ebb conditions of tidal water in mangroves of the Thane creek by simulating with varying spatial extends, bathymetry/topography, and different input parameters. The model results were compared and validated with the observed tide and currents data from January to February 2013. The modelled water level and current speed were well matching to the observed data. The model accurately represented semidiurnal spring and neap tides throughout the simulation period. The statistical parameters showed  $R^2 > 0.85$ ,  $IA > 0.8$ , and RMSE equal to 0.03 m on average at observation stations (Fig. 8, Fig. 9 and Table 3), which gives enough fidelity to model the real and experimental scenario.

The model has run for two scenarios, model *with* and *without mangroves*. The model simulation *with mangroves* accurately represents the flood and ebb water flow affected by the presence of mangroves. The maximum tidal elevation reached up to 2.4 m during spring tides and 1.9 m during neap tides at the head of the Thane creek (Supplementary Fig. 6). The tidal elevation is increasing from mouth to head of the creek. If the tidal elevation is greater than 2 m, the tidal water will reach all the mangrove areas through the channels radiating from the creek. When the tide recedes, a small amount of water remains in the mangroves. During the flood tide, the tidal currents showed a decreasing trend in the inundation regions (Figs. 10a and 11). Almost all regions have a tidal current of less than 0.5 m/s, and it reaches  $> 1$  m/s at some convergence zone of the creek (Supplementary Fig. 7). During both spring and neap tides, the tidal currents in the mangrove region were less than 0.2 m/s even though the maximum of 1 m/s were noticed near Vashi (Fig. 10a). Model *without mangroves* has been simulated for analysing the importance of mangroves on the hydrodynamics of Thane creek. In *without mangrove* simulation, Coastal inundation was severe with tidal currents greater than 0.7 m on average, and the tidal elevation has enhanced, and it exceeds 2.4 m (Figs. 10b and 12). Water stagnation was also noticed in the inundated regions during ebb tide (Fig. 12).

## **4. Discussion**

### **4.1 Status of mangroves around Thane creek**

Table 4 presented the comparison of the mangrove area estimated by the present study and other studies. The total area taken for these studies are different, but it showed consistency of increase in mangroves with the present study. Apart from all studies, FSI reported a dramatic increase in mangrove areas since 1987. The study by Prasad et al., (2010) found an increase in mangrove areas along the coastline from 1992 to 2001, while a decrease in the area from 2001 to 2005. Mallick et al., (2015) analysed a drastic reduction of mangroves (74.29 km<sup>2</sup>) between 1998 and 2003. Maharashtra state development report (2005) showed that the area under mangroves in Mumbai was 200 km<sup>2</sup> in 1972-75, which reduced to 108 km<sup>2</sup> in 1997 and finally increased to 118 km<sup>2</sup> in 2001. Vijay et al., (2020) also found an increase of 19.91 km<sup>2</sup> area of mangroves near Thane, Manori, and Malad creeks from 1972 to 2016. A recent study by IIST (2019) showed no considerable positive change in mangrove regions between 2009 and 2017. Only 11.02 km<sup>2</sup> area of mangroves increased, which might have been because of the urbanisation in Mumbai coastal regions. However, each study around Thane Creek shows a continuous increase in mangroves, with some decline in mangroves over the years. Mangroves may increase or decrease due to different climatic and anthropogenic activities. From 2000 onwards, the urbanisation and development activities concentrated on the coastal zones, specifically in the wetland and mangroves. The present study revealed that the increase in mangroves towards seaward

is more than that of landward. LULC map showed that the built-up area is more in the Thane than Karanja creek, causing seaward (Thane) and landward (Karanja) extension of mangroves. Development of industrial and residential sectors adjacent to the coastal areas restricts mangroves' growth towards the landward.

Most of the rivers in the Thane creek are used as drainages (Supplementary Table 1), and discharge of a large amount of solid waste and industrial effluents through these rivers display a negative impact on water circulation and quality of the Thane creek. The effect of the Ulhas river discharge (maximum of 1300 m/s during July) on Thane creek is marginal even though the freshwater input was higher because the average width of the Ulhas-Thane creek confluence is merely 50 m. These freshwater inputs were not sufficient to overcome the pollution around Thane creek. Increased pollution affects the growth and health of the mangrove forest very much adversely. The classification of mangrove species showed the dominance of the *Avicennia marina* along Thane creek; this species can survive in high salinity and pollution (including heavy metals lead, mercury, and chromium) conditions, which indicates that the increasing tendency of human activities on the landward side. The results of LULC and change detection revealed that mangroves in Mumbai coastal region are in the saturation stage, the stage at which the maximum growth of mangroves towards the landward region. This means that if there is any growth, it will only increase the mangrove towards the seaward or increase the quality of mangroves. Open and moderately dense mangroves may change to very dense mangroves or vice versa in the future. There is no further possibility of an increase in the area of mangroves to the land. Hence we can say that the mangroves of the Mumbai coast are in a saturation stage, and proper management plans should adopt to protect a healthy mangrove ecosystem concerning the life expectancy of the creek.

#### **4.2 Response of mangroves to the tidal dynamics**

The paper analyses the tidal dynamic response of Thane creek mangroves. The findings from the satellite imagery provide additional information, such as the extent of mangroves and the creek width, which will be considered when creating grids, friction coefficients, and land elevation. The geometry of the creek is almost triangular, which produces funnelling action during the flood tides and amplifies the tidal dynamics causing maximum tidal elevation at the head of the creek. Fig. 13 demonstrated a 25-day comparison of current speed during *with mangroves* and *without mangroves* at 3 locations (Karanja creek, Thane creek main channel west, and east), and it revealed that the presence of mangrove considerably reduces the maximum current speed from 1 m/s to less than 0.2 m/s. During *without mangrove* simulation, the tidal elevation has enhanced due to the perfect funnelling effect of the creek compared with the real situation; coastal inundation and tidal currents were higher during flood tide.

During such periods, the high tidal currents may erode sediments towards the longshore, cause instability to the coastal region, and, finally, threaten built-up areas and human settlements. The model simulation *with mangroves* showed decreased tidal currents in the inundation regions during high tide, where saline water covered all the mangrove species. When the tide recedes, a small amount of water remains in the mangroves due to friction and terrain slope. Analysis of satellite imageries from 1990 to 2017 revealed that the width of the Thane creek main channel has decreased and where tidal amplification showed an increasing trend. It is a vital phenomenon in estuaries and creeks where the depth and width gradually decrease; tidal amplification overcomes frictional dissipation of the energy. The decrease in the creek width confirms the deposition of sediment and increase of mangroves towards seaward, which also reduces the flow of tidal water, thereby increasing pollution (Vijay et al., 2020). Mallick et al., (2015) analysed erosion and deposition using satellite imagery around Thane creek and revealed that accretion is more prevalent than erosion. It may be due to the presence of mangroves that stabilise the coastal region. The existence of prominent mudflats along the creek indicates that dense mangroves significantly reduce erosional activity. When the tidal water moves through the mangroves, tidal attenuation occurs due to the friction, and these mangroves reduce the maximum magnitude of the tidal currents from 100 % to 20 % (1 m/s to 0.2 m/s). The mangroves attenuate a total of 80 % of tidal currents in the study region.

From 1990 to 2017, analysis from the mangrove classification and tidal model showed that mangroves in the Mumbai coast were increasing, which reduces tidal currents, while the tidal process controls the growth and distribution of mangrove species. Some of the mangrove species, especially the *Avicennia marina* of the Thane creek, always have water content concerning tidal activity. When tidal water enters the creek, flow reduces significantly due to mangrove vegetation. Even though reducing the tidal currents initiates erosion, sediments will transport and trap in the inundated region. This process becomes beneficial for the growth of mangrove species and thereby stabilises the coastal area of the creek.

### **4.3 Mangrove management strategy**

The present study highlights the application of satellite images to monitor about 100% increase in mangrove extent over three decades showing a favourable environment for its regeneration. From 1990 to 2017, Thane Creek's width decreased due to the seaward increase of mangroves and sedimentation with reduced tidal velocity (Fig. 13), causing the possibility of mangrove regeneration noticed from Fig. 5. But considering the permanence of the creek, the increase in mangroves towards the seaward gives a negative impact; a decrease in the creek width confirms the same. Therefore, we can say that the increase of mangroves in Thane creek towards seaward is a natural encroachment in favour of

urbanisation. In Mumbai, the growth of mangroves and urbanisation/anthropogenic activities follow a 1:2 ratio. The first one is for the area of increase in mangroves towards the seaward, and the second one is the area increase in urbanisation and anthropogenic activity adjacent to mangroves. LULC maps together with the ADCIRC model can be used to identify the inundated regions. The present modelling study substantiates such findings that the mangrove ecosystem significantly attenuates the magnitude of tidal current, causing sedimentation along the creek and further regeneration of mangroves. The model can run by extending for a longer interval of time to quantify the optimum sedimentation for the balanced mangrove-creek ecosystem. Hence understanding and estimating the cyclic processes of tidal attenuation, sedimentation, and mangrove regeneration in the estuarine or creek system will be valuable information for the sustainable management of mangroves and its ecosystem, however under-investigated for Indian mangroves. Complemented by integrating geospatial monitoring of the mangrove ecosystem using satellite remote sensing, it will be comprehensive for the long-term management of the creek system by management authorities. This study was an example of how to better understand a creek system by combining satellite imagery analysis and hydrodynamic modeling

#### **4.4 Importance and limitations of the study**

Several studies were conducted in the assessment of mangroves in Mumbai and other coastal regions (Sundarbans, Bhitarkanika, etc.) of India (Parida and Kumar, 2020; Parida and Kumari, 2021; Prasad et al., 2010; Roy et al., 2019; Sahana et al., 2019; Samant, 2002; SV et al., 2019; Vijay et al., 2005). The present study is consistent with other studies regarding the techniques adopted for classification and the outputs (LULC, mangrove extent, change detection, and species-level mapping). SMLC is the most effective and robust method of Mangroves classification based on traditional satellite remote sensing data (Dan et al., 2016). However, studies combining satellite and numerical modelling are limited. This will give an idea about how a mangrove ecosystem behaves in relation to tidal dynamics in a single frame. The LULC classification and the ADCIRC model would be useful to examine whether the tidal inundation threatens the built-up area. Generally, high-resolution (< 5 m) hyperspectral data are used for species-level classification, but it is also possible to classify mangrove species using sentinel-2 (Behera et al., 2021; Wang et al., 2019). Due to the limited availability of high-resolution spectral data, we focused on how to use freely available high-resolution satellite data (Sentinel-2) for species-level mapping. The present study is the first species classification of mangroves in Thane Creek using Sentinel-2. We have classified only four mangrove species with relatively low accuracy (66%) and K value (0.64). One of the limitations of the current study is the lack of *in-situ* data, which is the main reason for the decreased accuracy. To understand the magnitude of energy dissipated in the mangroves, the parameters such as sediment load, mangrove stem

configuration, roots, and branches diameter should be included during the ADCIRC model simulation, which was not achieved in the present study due to lack of *in-situ* data. Therefore, more ground truth data are mandatory in mangrove species classification and hydrodynamic model simulation.

## 5. Conclusion

Remote sensing provides a wide range of applications in wetland research and coastal water dynamics with a significant role in monitoring the mangrove ecosystem. In the present study, variation in the mangrove cover has been delineated from 1990 to 2017 and mapped the mangrove species (2017) distribution using satellite imagery, and it revealed that there is an overall increase in the area of mangroves, which is half of the increase in the built-up area. Anthropogenic pressure on landward mangroves may cause mangroves to expand further into the seaward. The dominance of *Avicennia marina* species indicates the severity of pollution and urbanisation. ADCIRC model simulation *with* and *without mangroves* gives the idea about the intensity of inundation. In *without mangroves*, tidal amplification increases to upstream due to the convergence along the channel, which intensifies tidal currents that enhance inundation and erosion, and finally end up with a threat to human settlements. Simulation *with mangroves* showed the reduction of tidal currents magnitude about 80% due to mangrove vegetation, thereby reducing the intensity of coastal inundation and stabilising the coast. Thus modified hydrodynamic conditions, in turn, control the growth and extent of the mangrove species in the tidal inundation regions. The study found that mangroves are in the saturation stage and have reached maximum growth towards land. Increased urbanisation limits the possibility of mangrove restoration in the land. The increase in mangroves towards seaward is reducing the creek width and finally questions the permanence of the creek considering the life expectancy. Decreasing the creek width also reduces the flow of tidal water and further increases pollution. The addition of mangrove extent information from satellite imagery to the hydrodynamic model provides maximum inundation and attenuation of tidal water. The LULC classification together with the ADCIRC model would be useful to test whether the tidal inundation is a threat to human beings. Therefore, the management authority should implement a proper management plan to monitor the mangroves and the anthropogenic activities in terms of mangrove restoration. The integrated satellite remote sensing for monitoring changes in mangroves and hydrodynamic model for assessing sediment accretion/erosion and inundation rates would be a promising set of tools to support the appropriate decision-making process for the restoration and conservation of mangroves. The findings from the study will be useful for the ecological conservation and restoration practices for the sustainable management of the mangrove-creek ecosystem that provides habitat for various terrestrial and aquatic fauna, including endangered species.

## **6. Acknowledgments**

The authors are thankful to the Director, NIO, Goa, and Scientist in Charge, NIO, Kochi, for providing the facilities throughout the paperwork writing. We are grateful to Dr V K Dadhwal, Director, IIST and Dr R. Jaishanker, Co-ordinator, Department of Ecological Informatics, IIITMK, Trivandrum, for the encouragement given during the work. The authors are thankful to the Naval Research Board (NRB, GAP 3168) for the financial assistance. We would also like to thank Crystal Fulcher, a Research Technician at UNC-IMS, for providing the ADCIRC source code.

## **7. Conflict of Interest**

The authors declare that they have no conflict of interest.

## **8. Ethical Statement**

This article does not contain any studies with human participants or animals performed by any of the authors.

## **9. Consent Statement**

For this type of study formal consent is not required.



## 10. References

- Alappatt, J.P., 2008. Structure and species diversity of mangrove ecosystem, in: *Biodiversity and Climate Change Adaptation in Tropical Islands*. Elsevier, pp. 127–144.
- Alongi, D.M., 2008. Mangrove forests: resilience, protection from tsunamis, and responses to global climate change. *Estuar. Coast. Shelf Sci.* 76, 1–13.
- Ambient, W.H.O., 2014. air pollution in cities database 2014. World Heal. Organ. Public Heal. Soc. Environ. Determ. Heal. Dep.
- Behera, M.D., Barnwal, S., Paramanik, S., Das, P., Bhattyacharya, B.K., Jagadish, B., Roy, P.S., Ghosh, S.M., Behera, S.K., 2021. Species-Level Classification and Mapping of a Mangrove Forest Using Random Forest—Utilisation of AVIRIS-NG and Sentinel Data. *Remote Sens.* 13, 2027.
- Blankespoor, B., Dasgupta, S., Lange, G.-M., 2017. Mangroves as a protection from storm surges in a changing climate. *Ambio* 46, 478–491.
- Bunt, J.S., Wolanski, E., others, 1980. Hydraulics and sediment transport in a creek-mangrove swamp system, in: *7th Australasian Conference on Hydraulics and Fluid Mechanics 1980: Preprints of Papers*. p. 492.
- Carugati, L., Gatto, B., Rastelli, E., Martire, M. Lo, Coral, C., Greco, S., Danovaro, R., 2018. Impact of mangrove forests degradation on biodiversity and ecosystem functioning. *Sci. Rep.* 8, 1–11.
- Census of India, 2011.
- Chapman, V.J., 1971. Mangroves v. tidal waves. *Biol Conserv* 4, 39.
- Chouksey, M.K., Kadam, A.N., Zingde, M.D., 2004. Petroleum hydrocarbon residues in the marine environment of Bassein--Mumbai. *Mar. Pollut. Bull.* 49, 637–647.
- Cohen, J., 1960. A coefficient of agreement for nominal scales. *Educ. Psychol. Meas.* 20, 37–46.
- Dahdouh-Guebas, F., Verheyden, A., De Genst, W., Hettiarachchi, S., Koedam, N., 2000. Four decade vegetation dynamics in Sri Lankan mangroves as detected from sequential aerial photography: a case study in Galle. *Bull. Mar. Sci.* 67, 741–759.
- Dan, T.T., Chen, C.F., Chiang, S.H., Ogawa, S., 2016. MAPPING AND CHANGE ANALYSIS IN MANGROVE FOREST BY USING LANDSAT IMAGERY. *ISPRS Ann. Photogramm. Remote Sens. Spat. Inf. Sci.* 3.
- Donato, D.C., Kauffman, J.B., Murdiyarso, D., Kurnianto, S., Stidham, M., Kanninen, M., 2011. Mangroves among the most carbon-rich forests in the tropics. *Nat. Geosci.* 4, 293–297.
- Duke, N.C., Meynecke, J.-O., Dittmann, S., Ellison, A.M., Anger, K., Berger, U., Cannicci, S., Diele, K., Ewel, K.C., Field, C.D., others, 2007. A world without mangroves? *Science (80- )*. 317, 41–42.
- Eastman, J.R., 2009. *IDRISI Taiga guide to GIS and image processing*. Clark Labs Clark Univ. Worcester, MA.

- Everard, M., Jha, R.R.S., Russell, S., 2014. The benefits of fringing mangrove systems to Mumbai. *Aquat. Conserv. Mar. Freshw. Ecosyst.* 24, 256–274.
- Everitt, J.H., Yang, C., Judd, F.W., Summy, K.R., 2010. Use of archive aerial photography for monitoring black mangrove populations. *J. Coast. Res.* 26, 649–653.
- Ferreira, M.A., Andrade, F., Bandeira, S.O., Cardoso, P., Mendes, R.N., Paula, J., 2009. Analysis of cover change (1995--2005) of Tanzania/Mozambique trans-boundary mangroves using Landsat imagery. *Aquat. Conserv. Mar. Freshw. Ecosyst.* 19, S38--S45.
- Forest Survey of India (FSI) Report, 2017.
- Geuzaine, C., Remacle, J.-F., 2009. Gmsh: A 3-D finite element mesh generator with built-in pre-and post-processing facilities. *Int. J. Numer. Methods Eng.* 79, 1309–1331.
- Ghosh, S.M., Behera, M.D., Paramanik, S., 2020. Canopy height estimation using sentinel series images through machine learning models in a Mangrove Forest. *Remote Sens.* 12, 1519.
- Giri, C., Pengra, B., Zhu, Z., Singh, A., Tieszen, L.L., 2007. Monitoring mangrove forest dynamics of the Sundarbans in Bangladesh and India using multi-temporal satellite data from 1973 to 2000. *Estuar. Coast. Shelf Sci.* 73, 91–100.
- Giri, C., Zhu, Z., Tieszen, L.L., Singh, A., Gillette, S., Kelmelis, J.A., 2008. Mangrove forest distributions and dynamics (1975--2005) of the tsunami-affected region of Asia. *J. Biogeogr.* 35, 519–528.
- Gnanappazham, L., Selvam, V., 2011. The dynamics in the distribution of mangrove forests in Pichavaram, South India--perception by user community and remote sensing. *Geocarto Int.* 26, 475–490.
- Hill, D., 2007. Tidal modeling of Glacier Bay, Alaska--Methodology, results and applications. Dep. Civil, Environ. Eng. Pennsylvania State Univ. Tech. Rep.
- Hindustan Times 13th July, 2015. Mumbai, mangroves act as a carbon sink.
- Indian Institute Of Space Science and Technology (IIST), 2019. Monitoring the health of mangroves of maharashtra state using near real time satellite remote sensing data.
- Kaliraj, S., Ch, N., 2012. Spectral recognition techniques and MLC of IRS P6 LISS III image for coastal landforms extraction along South West Coast of Tamilnadu, India. *Bonfring Int. J. Adv. Image Process.* 2, 1–7.
- Kantharajan, G., Pandey, P.K., Krishnan, P., Ragavan, P., Jeevamani, J.J.J., Purvaja, R., Ramesh, R., 2018. Vegetative structure and species composition of mangroves along the Mumbai coast, Maharashtra, India. *Reg. Stud. Mar. Sci.* 19, 1–8.
- Kathiresan, K., 2018. Mangrove forests of India. *Curr. Sci.* 114.
- Kathiresan, K., Rajendran, N., 2005. Coastal mangrove forests mitigated tsunami. *Estuar. Coast. Shelf Sci.* 65, 601–606.
- Kerr, A.M., Baird, A.H., 2007. Natural barriers to natural disasters. *Bioscience* 57, 102–103.

- Khawfany, A.A., Aref, M.A., Matsah, M.I., Taj, R.J., 2017. Utilizing Landsat-8 data in mapping of sabkha, mangroves, and land covers in Jizan coastal plain, southwestern Saudi Arabia. *Arab. J. Geosci.* 10, 103.
- Krishnamurthy, R.R., DasGupta, R., Chatterjee, R., Shaw, R., 2014. Managing the Indian coast in the face of disasters & climate change: a review and analysis of India's coastal zone management policies. *J. Coast. Conserv.* 18, 657–672.
- Landis, J.R., Koch, G.G., 1977. The measurement of observer agreement for categorical data. *Biometrics* 159–174.
- LeProvost database, <http://forum.aquaveo.com/topic/188-leprovost-database/>, 2008.
- Lu, G.Y., Wong, D.W., 2008. An adaptive inverse-distance weighting spatial interpolation technique. *Comput. Geosci.* 34, 1044–1055.
- Luetlich, R.A., Westerink, J.J., 1995. An assessment of flooding and drying techniques for use in the ADCIRC hydrodynamic model: Implementation and performance in one-dimensional flows. Contract Report, Prep. Headquarters, US Army Corps Eng. Vicksburg, MS.
- Maharashtra state development report, 2005.
- Mallick, P., Survase, R., Dhuri, M.S., 2015. Coastal Zone Analyses Around Mumbai--Thane Coast Using Multitemporal Satellite Data and Gis. *Int. J. Appl. Res.* 1, 936–946.
- Mandal, R.N., Naskar, K.R., 2008. Diversity and classification of Indian mangroves: a review. *Trop. Ecol.* 49, 131–146.
- Marois, D.E., Mitsch, W.J., 2015. Coastal protection from tsunamis and cyclones provided by mangrove wetlands--a review. *Int. J. Biodivers. Sci. Ecosyst. Serv. Manag.* 11, 71–83.
- Mas, J.F., 2004. Mapping land use/cover in a tropical coastal area using satellite sensor data, GIS and artificial neural networks. *Estuar. Coast. Shelf Sci.* 59, 219–230.
- Massel, S.R., Furukawa, K., Brinkman, R.M., 1999. Surface wave propagation in mangrove forests. *Fluid Dyn. Res.* 24, 219.
- Mazda, Y., Magi, M., Ikeda, Y., Kurokawa, T., Asano, T., 2006. Wave reduction in a mangrove forest dominated by *Sonneratia* sp. *Wetl. Ecol. Manag.* 14, 365–378.
- Mazda, Y., Magi, M., Kogo, M., Hong, P.N., 1997a. Mangroves as a coastal protection from waves in the Tong King delta, Vietnam. *Mangroves Salt marshes* 1, 127–135.
- Mazda, Y., Wolanski, E., King, B., Sase, A., Ohtsuka, D., Magi, M., 1997b. Drag force due to vegetation in mangrove swamps. *Mangroves salt marshes* 1, 193–199.
- Mitsch, W.J., Bernal, B., Hernandez, M.E., 2015. Ecosystem services of wetlands.
- Mitsch, W.J., Gosselink, J.G., Zhang, L., Anderson, C.J., 2009. Wetland ecosystems. John Wiley & Sons.

- Mujabar, P.S., Chandrasekar, N., 2013. Shoreline change analysis along the coast between Kanyakumari and Tuticorin of India using remote sensing and GIS. *Arab. J. Geosci.* 6, 647–664.
- Naidu, V.S., Sarma, R. V, 2001. Numerical modeling of tide-induced currents in Thane Creek, west coast of India. *J. Waterw. port, coastal, Ocean Eng.* 127, 241–244.
- Nayak, D., Balaji, R., 2016. Numerical modeling of tides, currents and waves off Maharashtra coast.
- Nayak, S., 2002. Use of satellite data in coastal mapping. *Indian Cartogr.* 22, 147–157.
- Neukermans, G., Dahdouh-Guebas, F., Kairo, J.G., Koedam, N., 2008. Mangrove species and stand mapping in Gazi Bay (Kenya) using Quickbird satellite imagery. *J. Spat. Sci.* 53, 75–86.
- Odum, W.E., McIvor, C.C., Smith III, T.J., 1982. The ecology of the mangroves of south Florida: a community profile.
- Parida, B.R., Kumar, P., 2020. Mapping and dynamic analysis of mangrove forest during 2009--2019 using landsat--5 and sentinel--2 satellite data along Odisha Coast. *Trop. Ecol.* 61, 538–549.
- Parida, B.R., Kumari, A., 2021. Mapping and modeling mangrove biophysical and biochemical parameters using Sentinel-2A satellite data in Bhitarkanika National Park, Odisha. *Model. Earth Syst. Environ.* 7, 2463–2474.
- Parida, B.R., Pandey, A.C., Patel, N.R., 2020. Greening and browning trends of vegetation in India and their responses to climatic and non-climatic drivers. *Climate* 8, 92.
- Patel, D.M., Patel, V.M., Bhupesh, K., Patel, K.A., 2014. Performance of mangrove in tsunami resistance. *Int. J. Emerg. Technol. Res.* 1, 29–32.
- Pattanaik, C., Reddy, C.S., Dhal, N.K., Das, R., 2008. Utilisation of mangrove forests in Bhitarkanika wildlife sanctuary, Orissa.
- Polidoro, B.A., Carpenter, K.E., Collins, L., Duke, N.C., Ellison, A.M., Ellison, J.C., Farnsworth, E.J., Fernando, E.S., Kathiresan, K., Koedam, N.E., others, 2010. The loss of species: mangrove extinction risk and geographic areas of global concern. *PLoS One* 5, e10095.
- Pradhan, M., Latkar, P., 2007. Shallow lakes in urban areas: ecological restoration of lakes in Thane City. *Proc. Taal* 1628–1634.
- Prasad, P., Pattanaik, C., Prasad, S.N., Dutt, C.B.S., 2010. Analysis of Spatial and Temporal Changes in Mangroves Along Thane Creek of Mumbai (India) Using Geospatial Tools. *IUP J. Environ. Sci.* 4, 52–59.
- QGIS Development Team (2018) QGIS Geographic Information System. Open Source Geospatial Foundation Project. <http://qgis.osgeo.org>".
- Rakotomavo, A., Fromard, F., 2010. Dynamics of mangrove forests in the Mangoky River delta, Madagascar, under the influence of natural and human factors. *For. Ecol. Manage.* 259, 1161–1169.
- Regression, G.W., 2016. Help| ArcGIS for Desktop [Internet]. Desktop. [arcgis.com](http://arcgis.com).

- Richards, J.A., 2013. Supervised classification techniques, in: *Remote Sensing Digital Image Analysis*. Springer, pp. 247–318.
- Roy, A., 2019. Making India's coastal infrastructure climate-resilient: challenges and opportunities. *Obs. Res. Found.*
- Roy, S., Mahapatra, M., Chakraborty, A., 2019. Mapping and monitoring of mangrove along the Odisha coast based on remote sensing and GIS techniques. *Model. Earth Syst. Environ.* 5, 217–226.
- Sahana, M., Dutta, S., Sajjad, H., 2019. Assessing land transformation and its relation with land surface temperature in Mumbai city, India using geospatial techniques. *Int. J. Urban Sci.* 23, 205–225.
- Sahu, S.C., Suresh, H.S., Murthy, I.K., Ravindranath, N.H., 2015. Mangrove area assessment in India: implications of loss of mangroves. *J. Earth Sci. Clim. Change* 6, 1.
- Samant, H.P., 2002. Quantifying mangrove cover change in and around Mumbai using satellite data, in: *Proceedings of the National Seminar on Creeks, Estuaries and Mangroves- Pollution and Conservation*, 28 Th to 30 Th November, 2002, Thane. pp. 334–337.
- Sastry, J.S., 1971. The mechanism of sediment transport in the environs of Bombay harbour, in: *Proceedings of the Symposium on the Engineering Properties of Sea-Floor Soils and Their Geophysical Identification*. pp. 338–349.
- Selvam, V., Ravichandran, K.K., Gnanappazham, L., Navamuniyammal, M., 2003. Assessment of community-based restoration of Pichavaram mangrove wetland using remote sensing data. *Curr. Sci.* 794–798.
- Shelestov, A., Lavreniuk, M., Kussul, N., Novikov, A., Skakun, S., 2017. Exploring Google Earth Engine platform for big data processing: Classification of multi-temporal satellite imagery for crop mapping. *Front. Earth Sci.* 5, 17.
- Short, A.D., Trembanis, A.C., 2004. Decadal scale patterns in beach oscillation and rotation Narrabeen Beach, Australia—time series, PCA and wavelet analysis. *J. Coast. Res.* 20, 523–532.
- Spalding, M., McIvor, A., Tonneijck, F., Tol, S., Eijk, P. van, 2014. Mangroves for coastal defence.
- SV, S., Vethamony, P., Bhaskaran, P.K., Pednekar, P., Jishad, M., James, R.A., 2019. Attenuation of wave energy due to mangrove vegetation off Mumbai, India. *Energies* 12, 4286.
- Tam, N.F.Y., Wong, Y.S., 1999. Mangrove soils in removing pollutants from municipal wastewater of different salinities. *J. Environ. Qual.* 28, 556–564.
- The Energy and Resources Institute (TERI), 2015. Environmental status report by Mumbai metropolitan region development authority (MMRDA).
- Thomas, J., Velamala, S.N., Prasad, K., 2019. Numerical simulation of tidal constituents in Thane Creek and the Ulhas Estuary, West Coast of India. *J. Coast. Res.* 35, 376–388.
- Tomlinson, P.B., 2016. *The botany of mangroves*. Cambridge University Press.

- Tomlinson, P.B., 1986. *the Botany of Mangroves* Cambridge University Press London.
- United Nations report, 2012.
- Van Loon, A.F., Te Brake, B., Van Huijgevoort, M.H.J., Dijkma, R., 2016. Hydrological classification, a practical tool for mangrove restoration. *PLoS One* 11, e0150302.
- van Maanen, B., Coco, G., Bryan, K.R., 2015. On the ecogeomorphological feedbacks that control tidal channel network evolution in a sandy mangrove setting. *Proc. R. Soc. A Math. Phys. Eng. Sci.* 471, 20150115.
- Vijay, R., Dey, J., Sakhre, S., Kumar, R., 2020. Impact of urbanization on creeks of Mumbai, India: a geospatial assessment approach. *J. Coast. Conserv.* 24, 1–16.
- Vijay, R., Khobragade, P.J., Sohony, R.A., Kumar, R., Wate, S.R., 2014. Hydrodynamic and water quality simulation of Thane creek, Mumbai: an impact of sewage discharges.
- Vijay, V., Biradar, R.S., Inamdar, A.B., Deshmukhe, G., Baji, S., Pikle, M., 2005. Mangrove mapping and change detection around Mumbai (Bombay) using remotely sensed data.
- Wang, L., Jia, M., Yin, D., Tian, J., 2019. A review of remote sensing for mangrove forests: 1956--2018. *Remote Sens. Environ.* 231, 111223.
- Wang, L., Sousa, W.P., Gong, P., 2004. Integration of object-based and pixel-based classification for mapping mangroves with IKONOS imagery. *Int. J. Remote Sens.* 25, 5655–5668.
- Wang, Y., Bonyng, G., Nugranad, J., Traber, M., Ngusaru, A., Tobey, J., Hale, L., Bowen, R., Makota, V., 2003. Remote sensing of mangrove change along the Tanzania coast. *Mar. Geod.* 26, 35–48.
- WCMC, U., n.d. Shoreline protection and other ecosystem services from mangroves and coral reefs.
- Wells, S., Ravilious, C., 2006. In the front line: shoreline protection and other ecosystem services from mangroves and coral reefs. *UNEP/Earthprint*.
- Youdon, C., 2020. Climate change impact on mangrove ecosystems in India's coastal regions. *Natl. Marit. Found.* 8–60.
- Zhang, K., Liu, H., Li, Y., Xu, H., Shen, J., Rhome, J., Smith III, T.J., 2012. The role of mangroves in attenuating storm surges. *Estuar. Coast. Shelf Sci.* 102, 11–23.
- Zhang, Y., 2011. Coastal environmental monitoring using remotely sensed data and GIS techniques in the Modern Yellow River delta, China. *Environ. Monit. Assess.* 179, 15–29.
- Zingde, M.D., Bhosle, N.B., Narvekar, P. V, Desai, B.N., 1989. *Hydrography and water quality of Bombay harbour*. Muzaffarnagar: Society of Biosciences.

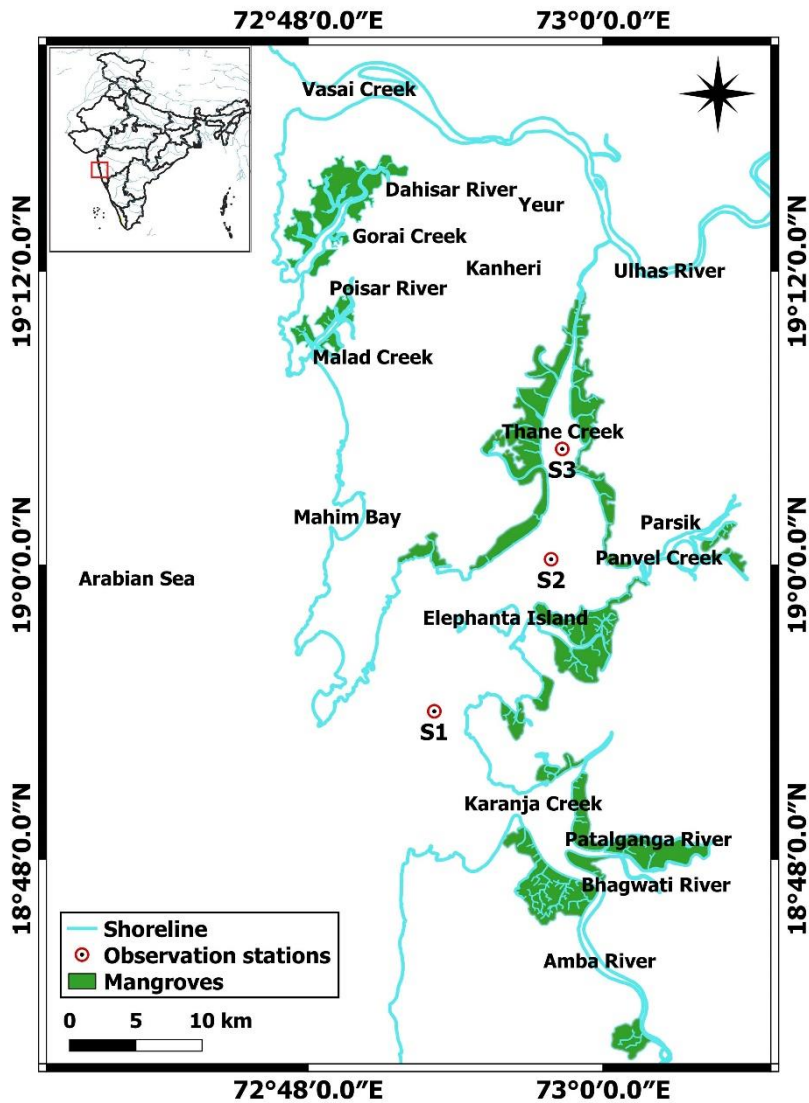


Fig. 1. Study area encompassing Thane creek, Mumbai including small creeks, rivers and mangroves, and observation stations (S1, S2 and S3).

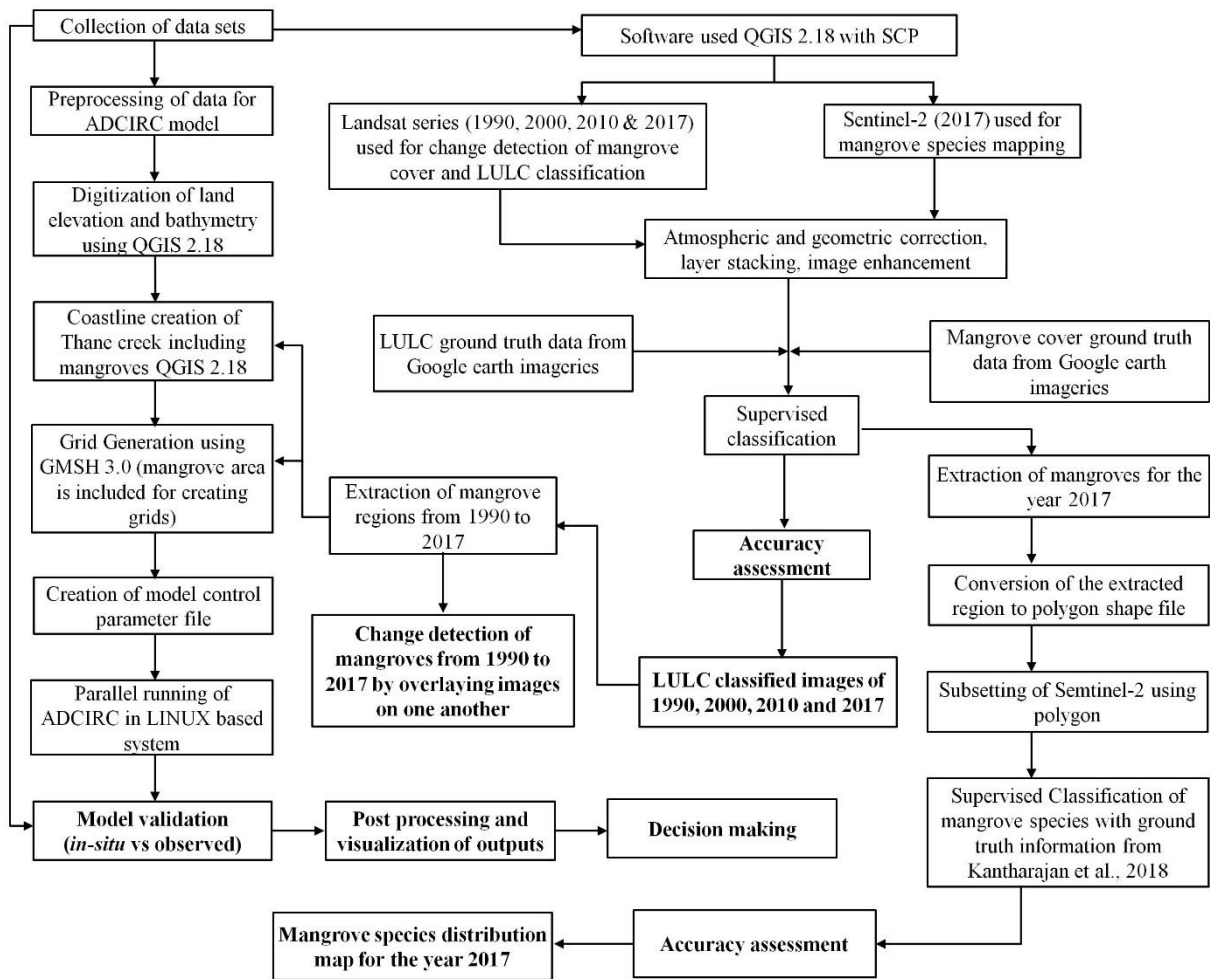


Fig. 2. Flow diagram for the simulation of ADCIRC model, Change detection of Mangroves, LULC classification and Mangrove species distribution.



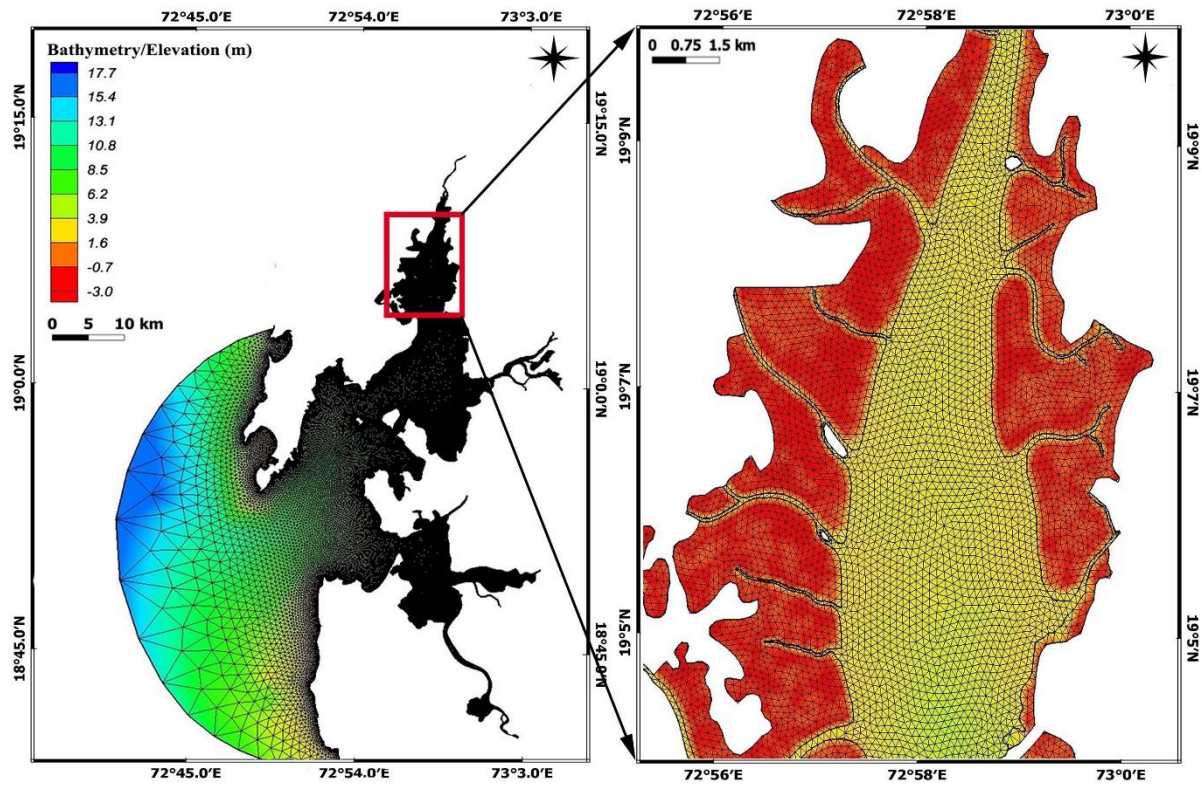


Fig. 3. Unstructured grid developed for Thane creek, Mumbai (left) and mangrove ecosystem in the red shade (right)

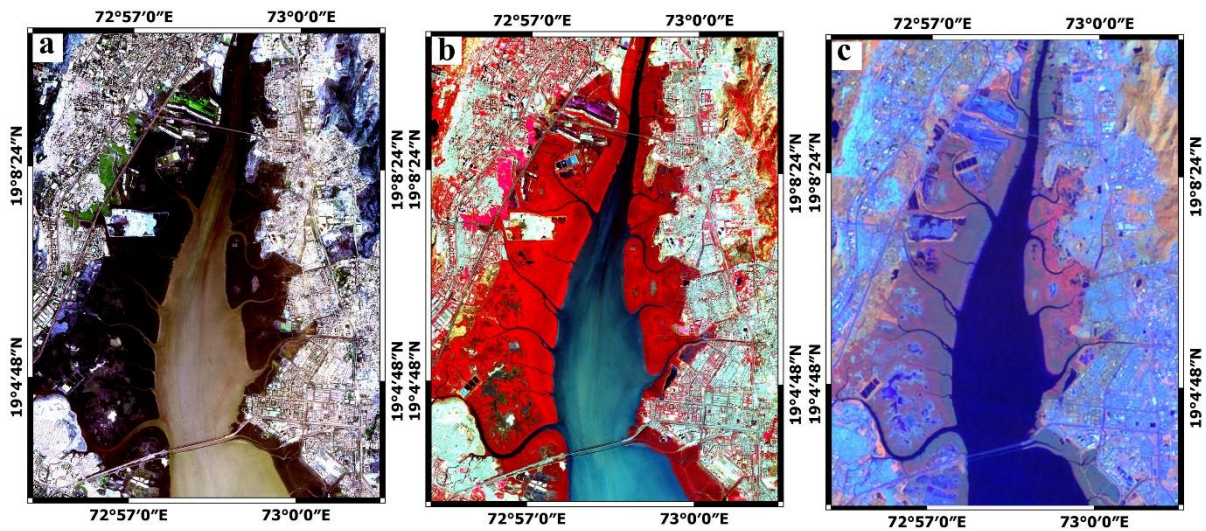


Fig. 4. Band Combination of Landsat-7 series for the year 2010: (a) True color composite (R-B-G), (b) false-color composite (SWIR1-R-G), and (c) false-color composite (NIR-SWIR1-TIR).

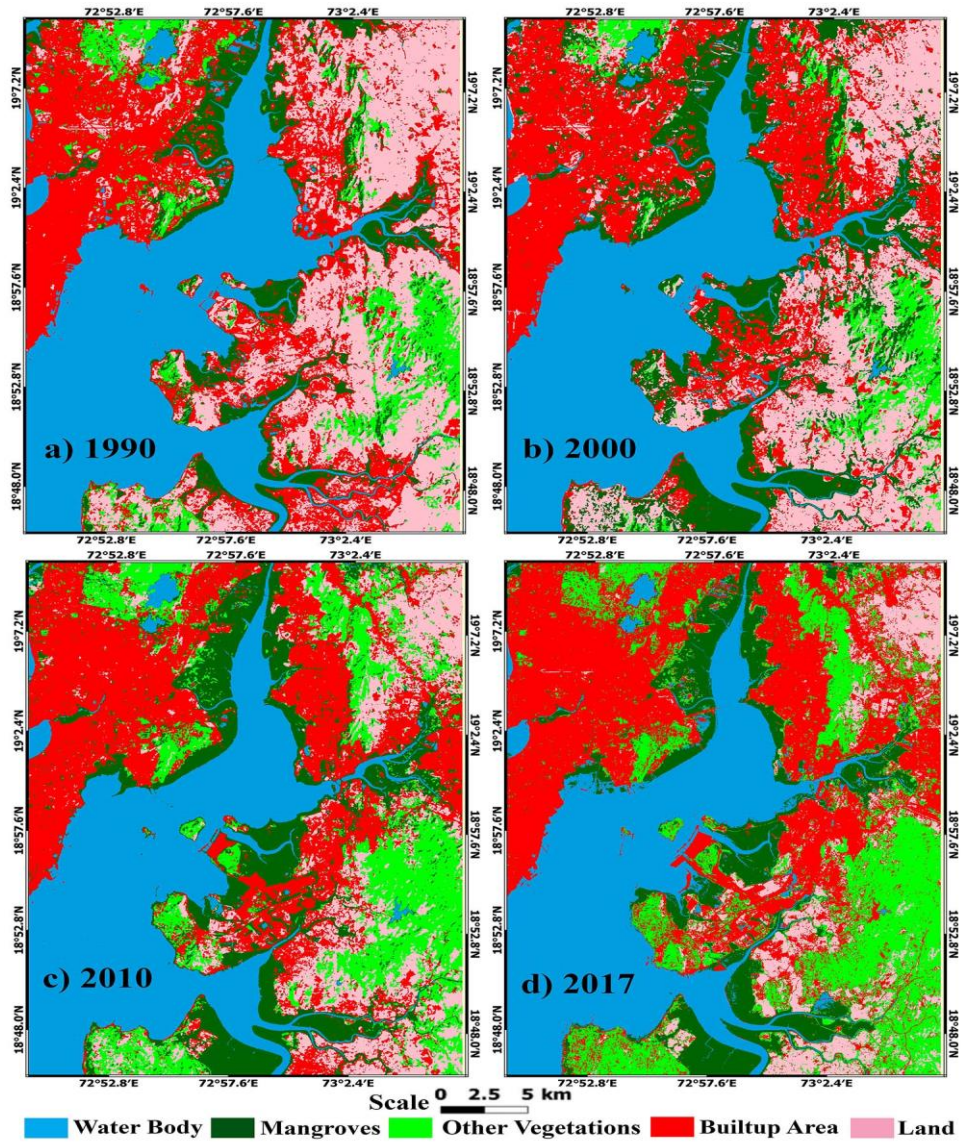


Fig. 5. LULC classification of Thane creek, Mumbai for the years a) 1990, b) 2000, c) 2010 and d) 2017.

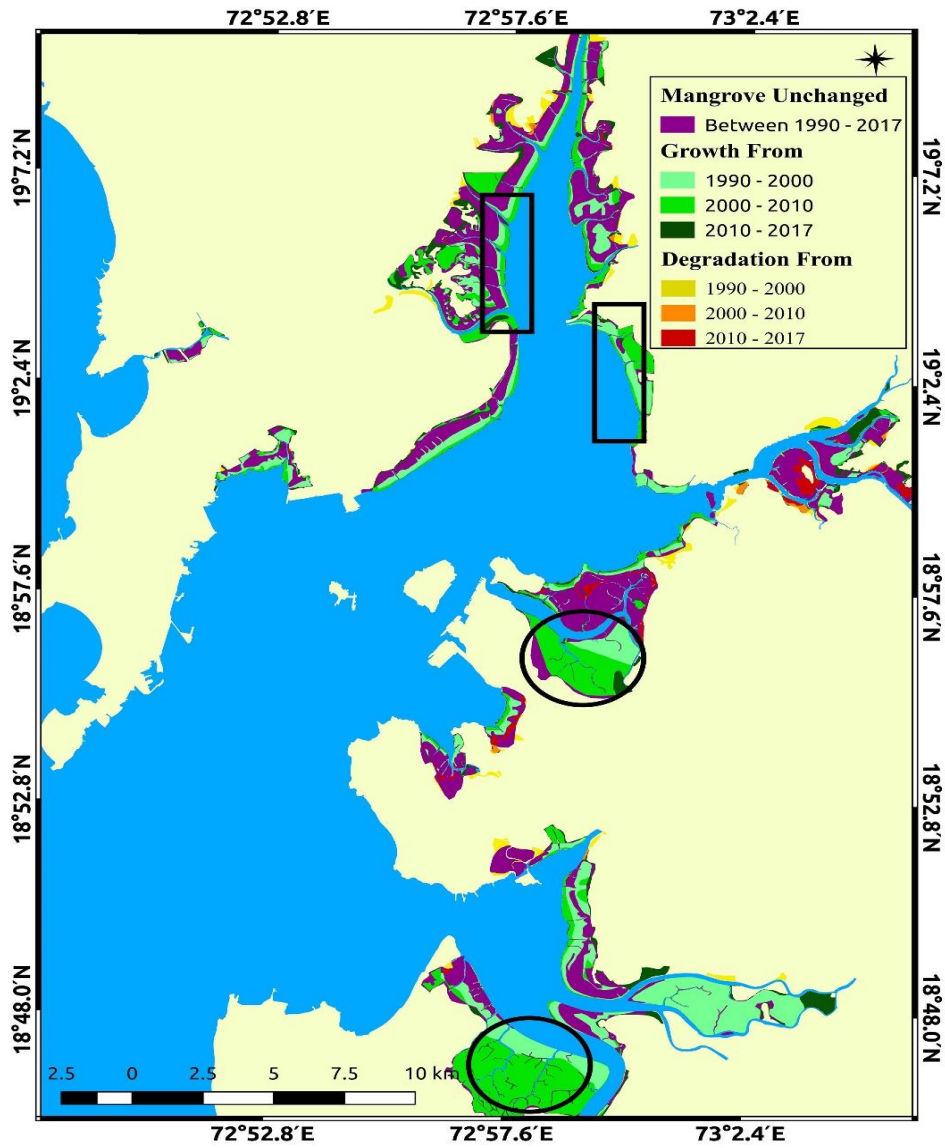


Fig. 6. Mangrove cover of Thane creek, Mumbai from 1990 to 2017. Major landward (circle) and seaward (rectangular box) growth of mangroves were demarcated.

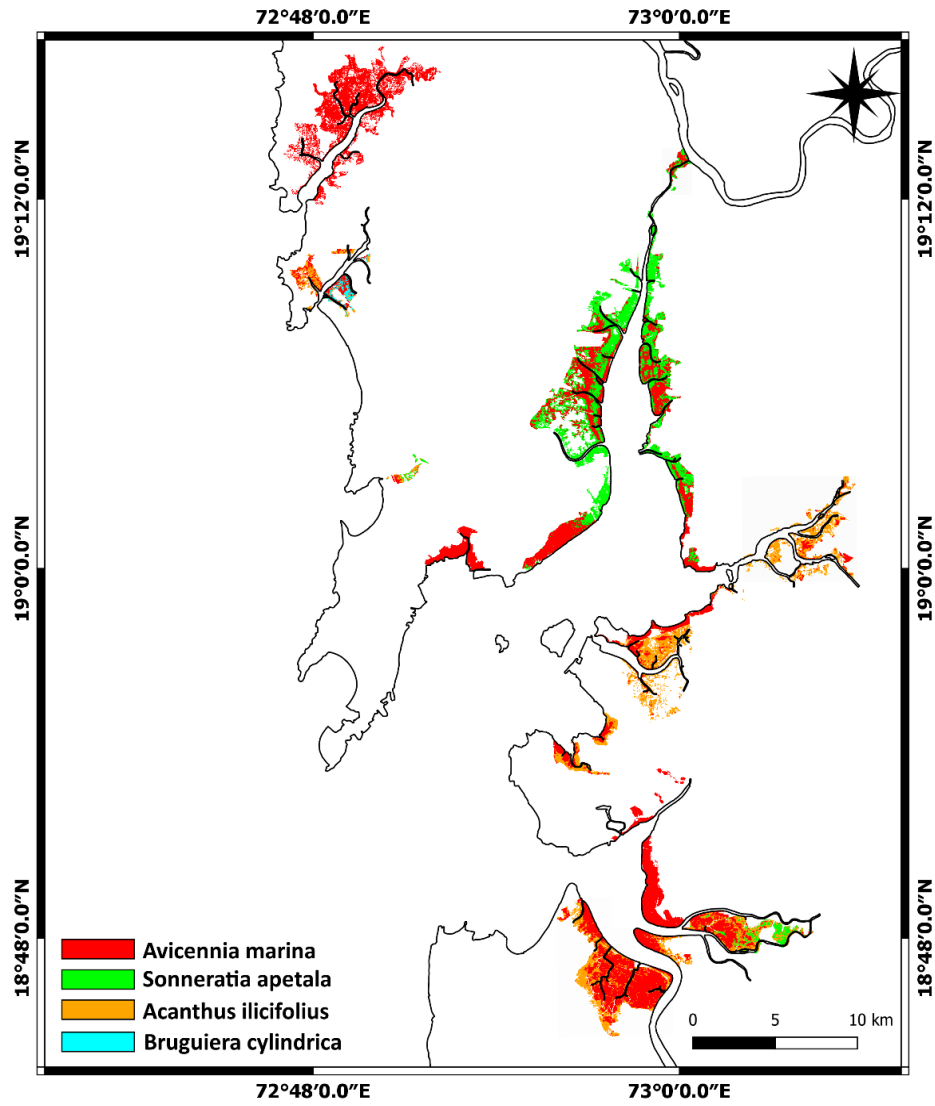


Fig. 7. Mangrove species distribution in Thane creek, Mumbai during 2017.

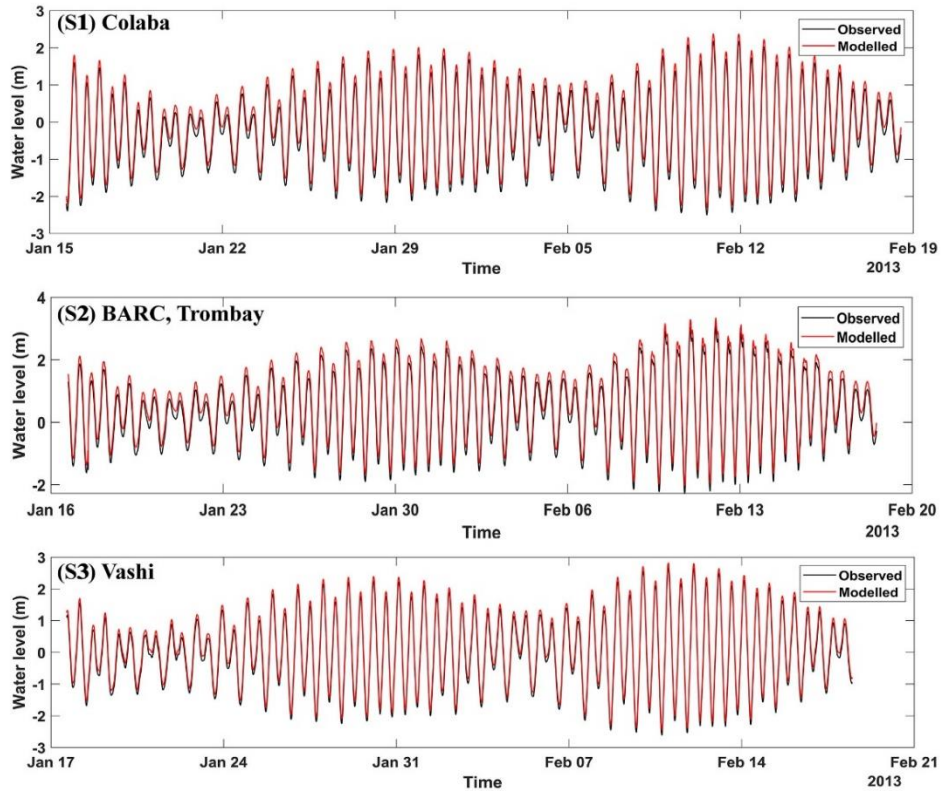


Fig. 8. Comparison of model-predicted and observed water level at three locations (S1, S2 and S3).

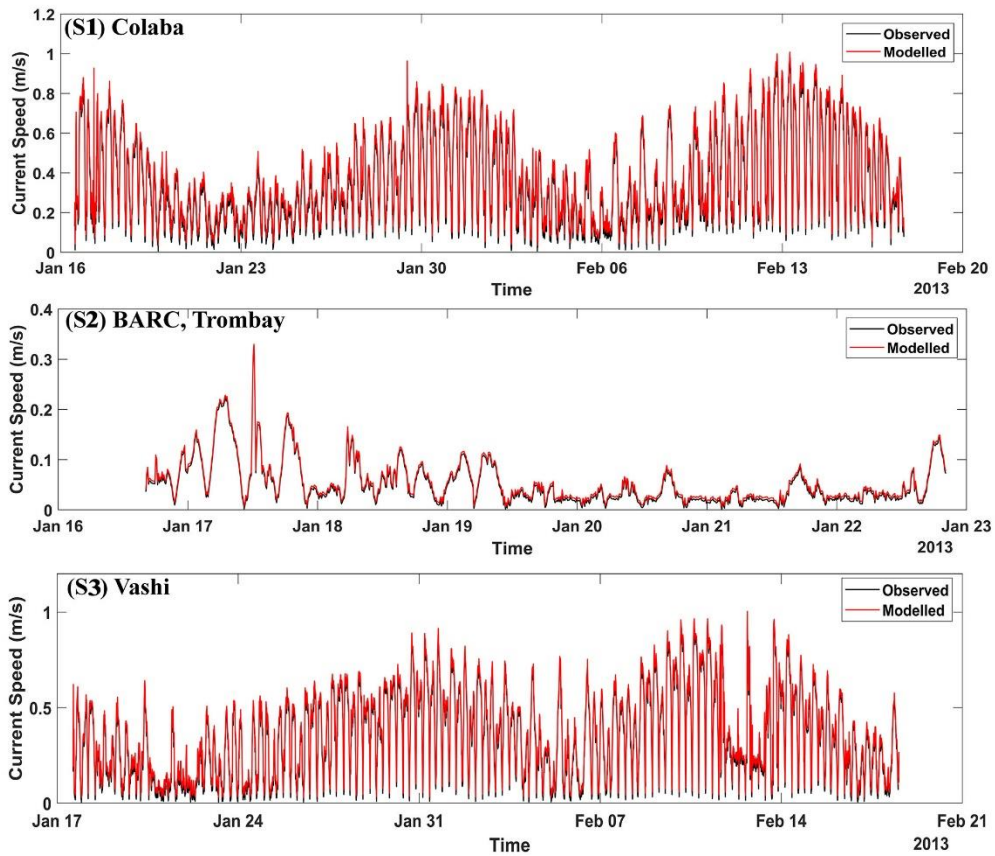


Fig. 9. Comparison of model-predicted and observed current speed at three locations (S1, S2 and S3).

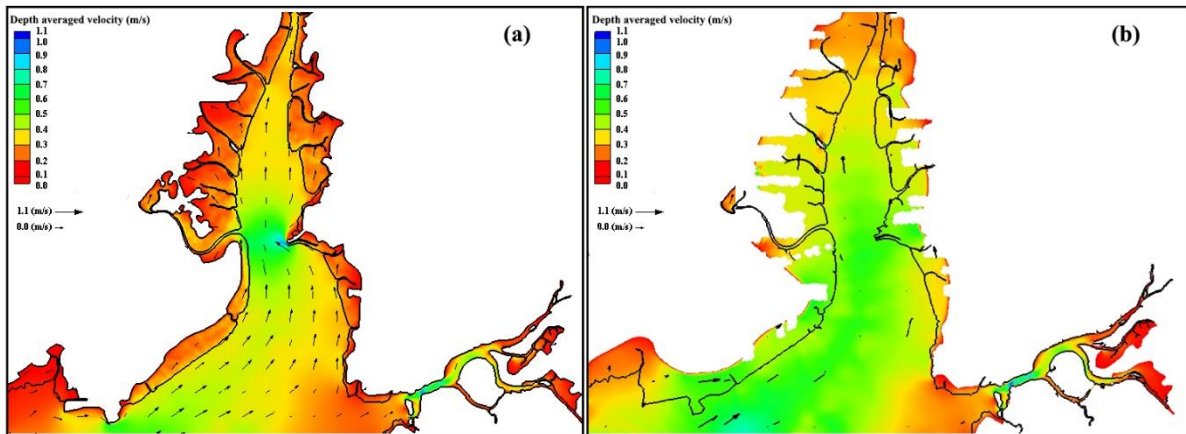


Fig. 10. Tidal current and attenuation of water flow in Thane creek, Mumbai a) *with mangroves* and b) *without mangroves*

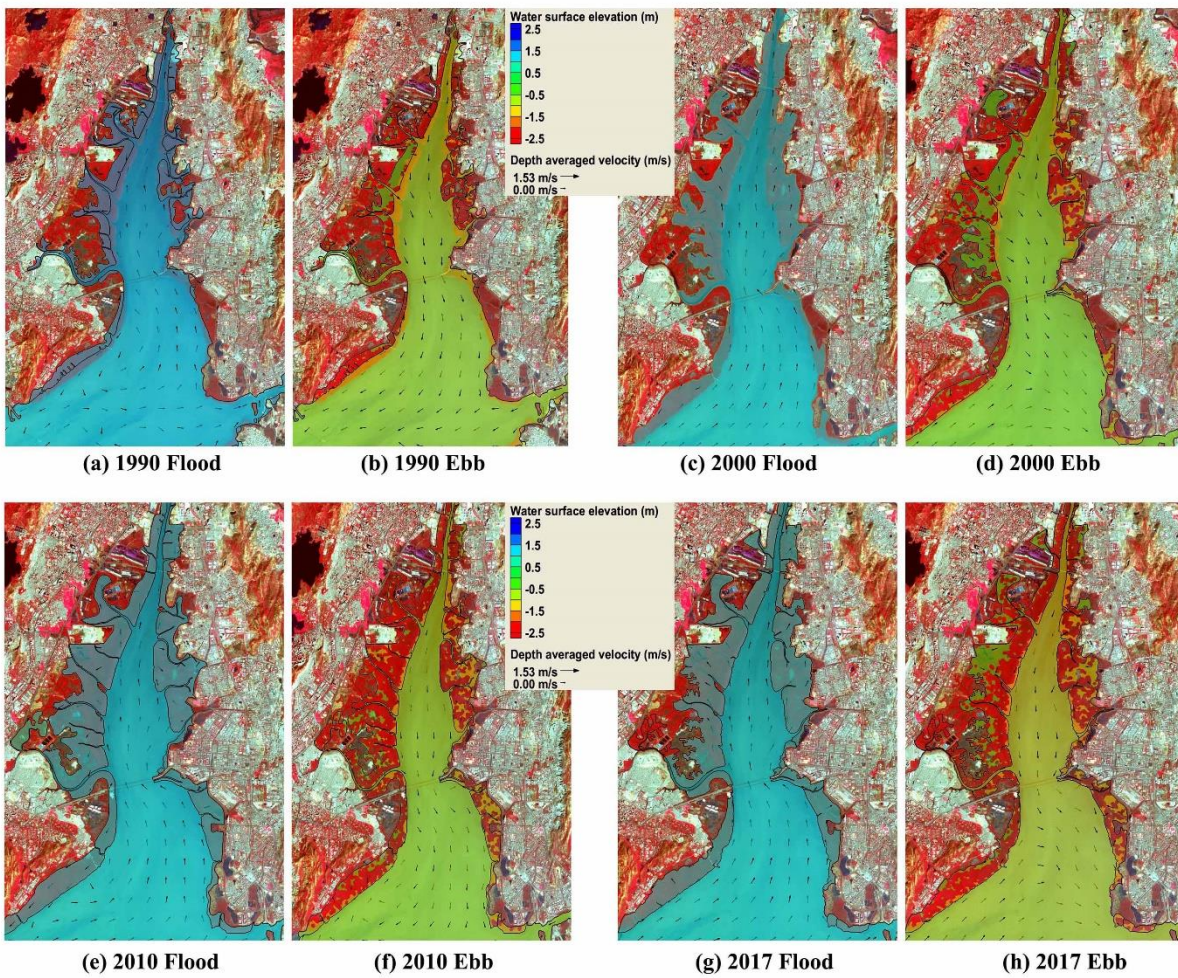


Fig. 11. Flood and Ebb condition of Thane creek main channel (*with mangroves*) from 1990 to 2017.

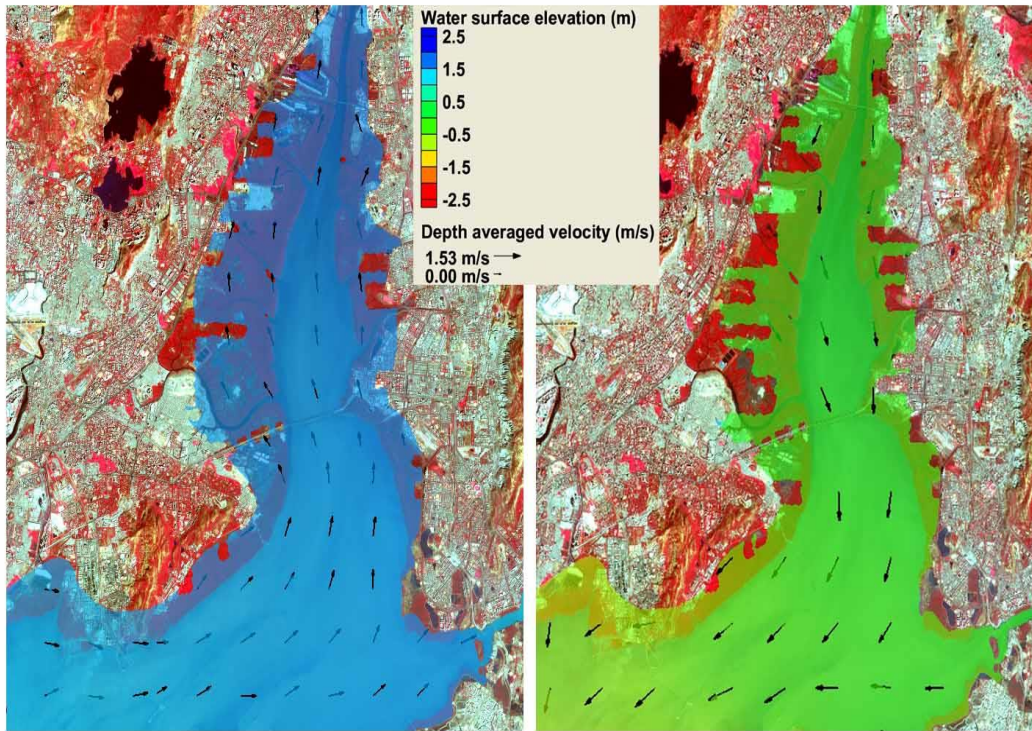


Fig. 12. Flood (left) and Ebb (right) condition of Thane creek main channel *without mangroves* for the year 2017.

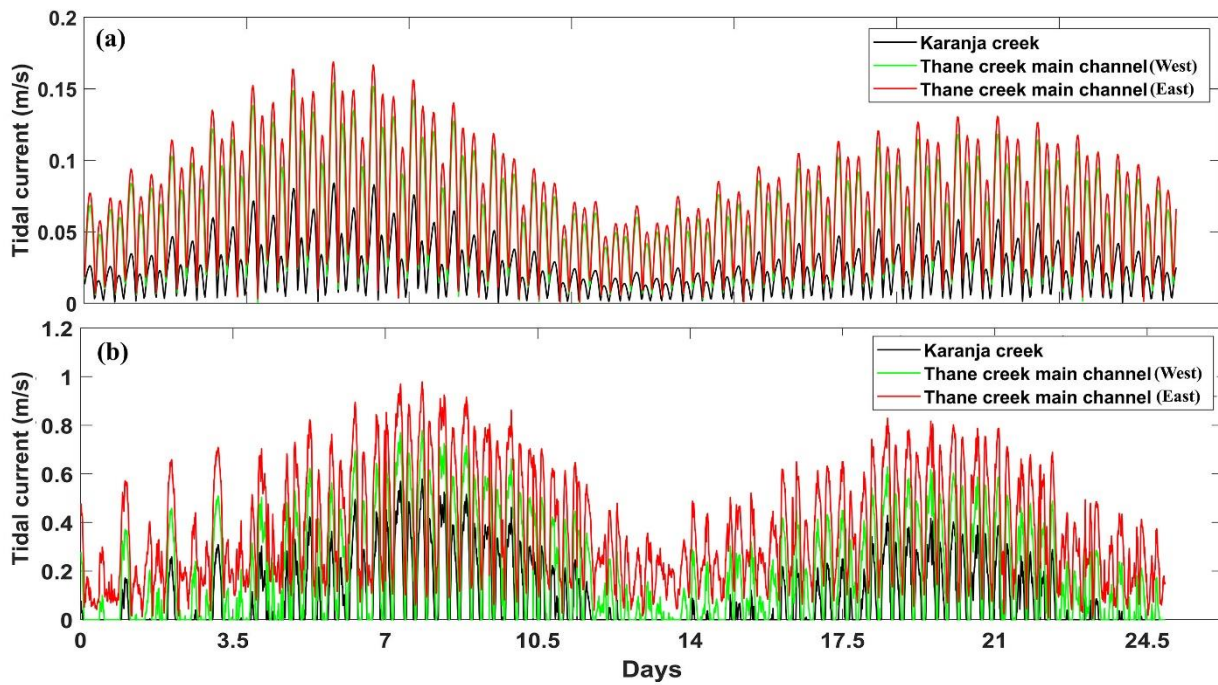


Fig. 13. Graphical representation of tidal current at three locations of Thane creek, Mumbai a) *with mangroves* b) *without mangroves*.

Table 1. Details of different datasets used for the study

<b>Data</b>	<b>Spatial Resolution</b>	<b>Satellite data Acquisition (dd/mm/yyyy)</b>	<b>Source</b>
Landsat 5 TM	30 meter	09/03/1990	USGS
Landsat 7 ETM	30 meter (15 meter for band 8)	25/02/2000	USGS
Landsat 7 ETM	30 meter (15 meter for band 8)	08/03/2010	USGS
Landsat 8 OLI	30 meter (100 meter for band 10 and 11 and 15 meter for band 8)	03/03/2017	
SENTINEL-2 MSI	Band 2, 3, 4 and 8 have 10 meters, Band 5, 6, 11, 12 have 20 meters, for band 1, 9, 10 have 60 meters.	12/02/2017	USGS
SRTM	30 meter	23/09/2014	USGS
CARTOSAT-1	2.5 meter	29/04/2015	ISRO-BHUVAN
Gridded Bathymetry data	~1000 meter	2014	GEBCO
Gridded Bathymetry data	~2000 meter	2014	GEBCO
High-resolution bathymetric charts (21 charts)	910 (1:10000), 911 (1:5000), 912 (1:5000), 913 (1:5000) ,1142 (1:10000), 1330 (1:5000), 1330A (1:10000), 1334 (1:5000), 1335 (1:5000), 1336 (1:5000), 1337 (1:5000), 1377 (1:2500), 1378 (1:2500), 1379 (1:5000), 1380 (1:5000) , 1381 (1:5000) , 1382 (1:5000) , 1383 (1:5000) , 1384 (1:5000) , 1396 (1:10000), 1401 (1:10000)	2009 to 2012	Maharashtra Maritime Board (MMB)



Table 2. Accuracy assessment of classified images

Year	Average Accuracy (%)	Kappa Coefficient (K)
1990 (LULC)	87	0.79
2000 (LULC)	88	0.86
2010 (LULC)	93	0.91
2017 (LULC)	94	0.93
2017 (Mangrove species)	66	0.64

Table 3. Validation of modelled data against *in-situ* observation (Correlation coefficient squared ( $R^2$ ), Index of agreement (IA), and root mean square error (RMSE)).

Stations	Water Level			Current Speed		
	$R^2$	RMSE (m)	Index of Agreement	$R^2$	RMSE (m)	Index of Agreement
Colaba (S1)	0.87	0.04	0.91	0.85	0.05	0.82
BARC Trombay (S2)	0.92	0.02	0.95	0.91	0.02	0.89
Vashi (S3)	0.88	0.03	0.93	0.86	0.04	0.83

Table 4. Comparison of mangrove area estimated by this study and other studies

<b>Studies (regions)</b>	<b>Mangrove area change in km<sup>2</sup> (years)</b>
This study (Thane, Mumbai City, Mumbai Suburban)	79.14, 111.52, 144.82 and 154.5 (1990, 2000, 2010 and 2017)
Prasad et al., 2010 (Thane)	34.4, 47.7 and 42.9 (1992, 2001 and 2005)
Mallick et al. 2015 (Thane, Mumbai City, Mumbai Suburban, Vasai creek)	201.74, 127.45, 204.56 and 223 (1998, 2003, 2008 and 2011)
Maharashtra state development report, 2005	200, 108 and 118 (1972, 1997 and 2001)
FSI (Thane, Mumbai city, Mumbai Suburban), 2017	45, 75, 98 to 156 (1987, 2001, 2011 and 2017)
Indian Institute of Space Science and Technology (IIST), annual report 2019 (Thane and Mumbai-Suburban)	108.77, 111.37 and 119.79 (2009, 2014 and 2017)
Vijay et al., 2020 (Thane, Malad and Manori)	72.59, 77.07 and 92.5 (1972, 1994 and 2016)